Front. Electr. Electron. Eng. 2012, 7(4): 416–426
DOI 10.1007/s11460-012-0219-6

RESEARCH ARTICLE

Yashar HASHEMI, Rasool KAZEMZADEH, Mohammad Reza AZIZIAN, Ahmad SADEGHI YAZDANKHAH

Improving power system dynamic performance using attuned design of dual-input PSS and UPFC PSD controller

Abstract The objective of this work is the coordinated design of controllers that can enhance damping of power system swings. With presence of flexible AC transmission system (FACTS) device as unified power flow controller (UPFC), three specific classes of the power system stabilizers (PSSs) have been investigated. The first one is a conventional power system stabilizer (CPSS); the second one is a dual-input power system stabilizer (dual-input PSS); and the third one is an accelerating power PSS model (PSS2B). Dual-input PSS and PSS2B are introduced to maintain the robustness of control performance in a wide range of swing frequency. Uncoordinated PSS and UPFC damping controller may cause unwanted interactions; therefore, the simultaneous coordinated tuning of the controller parameters is needed. The problem of coordinated design is formulated as an optimization problem, and particle swarm optimization (PSO) algorithm is employed to search for optimal parameters of controllers. Finally, in a system having a UPFC, comparative analysis of the results obtained from application of the dual-input PSS, PSS2B, and CPSS is presented. The eigenvalue analysis and the time-domain simulation results show that the dual-input PSS & UPFC and the PSS2B & UPFC coordination provide a better performance than the conventional single-input PSS & UPFC coordination. Also, the PSS2B & UPFC coordination has the best performance.

Keywords simultaneous coordinated design, unified power flow controller (UPFC), power swing damping (PSD), dual-input power system stabilizer

Received August 26, 2012; accepted October 16, 2012

Yashar HASHEMI, Rasool KAZEMZADEH (✉),
Mohammad Reza AZIZIAN, Ahmad SADEGHI YAZDANKHAH
Faculty of Electrical Engineering, Sahand University of Technology, Tabriz, Iran
E-mail: r.kazemzadeh@sut.ac.ir

1 Introduction

Power systems contain many modes of swing as a consequence of interactions of its components, e.g., one generator rotor swinging relative to another. The frequencies of these swings are usually in the range of 0.2–3 Hz [1]. There are two electromechanical (EM) modes of swings to be considered [2]: a) local mode with a frequency of 0.8–3 Hz, which is related to swing in a single generator or a group of generators in the same area against each other; and b) inter area mode with frequency of 0.2–0.8 Hz, in which the units in one area oscillate against those in other area. The lack of sufficient damping could lead to power transfer restrictions and in extreme cases power system collapse.

Traditionally, the damping of low frequency swings is provided by putting in a power system stabilizer (PSS) which uses local measurement signals such as rotor speed or active power as feedback signals. Among generator exciter control procedures for stability enhancement [3–5], PSS-based active power is used as the input signal in numerous cases. These procedures damp out the local power swings between generators. With regard to minor information contained in active power signal, damping of low frequency power system swings is non-significant by this procedure. To solve this disadvantage of conventional PSS, rotor speed deviation is used as the input signal [3,4]. These two signals are gathered after passing through compensators, and the resultant signal is applied to PSS that can vastly improve stability. Accelerating power PSS model (PSS2B) [6] is the other model of the dual-input stabilizer which uses combinations of power and speed signals to derive the stabilizing signal. In this type of PSS, there is no need for a torsional filter in the main stabilizing path. This eliminates the exciter mode stability problem, thereby permitting a higher stabilizer gain that results in better damping of system swings.

Another effective way to damp power system swings is

the use of flexible AC transmission system (FACTS) devices, which is a genetic term for a group of technologies that radically increase the capacity of the transmission network while maintain or improve voltage stability and grid reliability. This type of damping control is realized by adding a supplementary stabilizing signal on the primary control loops of FACTS devices. In these cases, FACTS power swing damping (PSD) controllers are effective solutions, where damping power swing with FACTS devices is affected through power modulation by a supplementary damping controller (SDC) and is called a FACTS device stabilizer (FDS) [7].

Many approaches have been adopted to design the FACTS controllers. Several approaches based on modern control theory have been applied to thyristor controlled series compensation (TCSC) controller design. Chang and Chow [8] developed a time optimal control strategy for the TCSC where a performance index of time was minimized. Heuristic optimization techniques and modified particle swarm optimization (PSO) have been implemented to search for the optimum TCSC-based stabilizer parameters for the purpose of enhancing single-machine infinite bus (SMIB) system stability [9–11]. A considerable attention has been directed to the realization of various thyristor controlled phase shifter (TCPS) schemes. Baker et al. [12] have developed a control algorithm for static phase shifting transformer using stochastic optimal control theory, and Jiang et al. [13] have proposed a static phase shifting transformer control technique based on nonlinear variable structure control theory. In the literature, static var compensators (SVCs) have been applied for enhancing the stability performance of power systems [14]. Robust SVC controller based on H_∞, structured singular value μ, and quantitative feedback theory (QFT) also has been presented to enhance system damping [15–17]. Research on the possible damping effect of unified power flow controller (UPFC), the most versatile FACTS device, has also been conducted during the recent years. Besides the works in Refs. [18,19], Dong et al. [20] have proposed a PI-based approach for the dynamic control of UPFC. In Ref. [21], a fuzzy logic based damping controller for UPFC has been developed, and the effectiveness of this fuzzy controller has been demonstrated in the simulation results of a two-area four-machine system.

However, uncoordinated local control of FACTS devices and PSSs may cause unwanted interactions that further results in the system destabilization. To improve overall system performance, many researches have been made on the coordination among conventional PSS and FACTS PSD controller [22–25]. Some of these methods are based on the complex nonlinear simulation [22,23], and the others are linear approaches [24,25].

A comparative analysis between the results from application of the PSS2B, dual-input PSS, and conventional power system stabilizer (CPSS) in coordination with the UPFC as a FACTS device is presented in this paper. The problem of robust output feedback controller coordinated design is formulated as an optimization problem and PSO algorithm is employed to search for optimal parameters of controllers. First, the system eigenvalues without controllers and then with the proposed controllers are investigated. It is quite evident from the results that the system stability is greatly enhanced with the coordinated design of dual-input PSS & UPFC and PSS2B & UPFC as the damping ratio of the electromechanical mode eigenvalue has been greatly improved. In this study, the nonlinear time-domain simulation is carried out using MATLAB software to validate the effectiveness of the proposed controllers. The controllers are simulated and tested under different operating conditions.

2 Model of power system including UPFC

To design a damping controller by using the proposed method, an SMIB system has been used in this research. First, dynamic equations of SMIB system with UPFC are gained that include the following stages:

- Obtaining the dominant equations of the system.
- Identifying the state variables of the system.
- Calculating the electric parameters in each operating point.
- Linearizing the dominant equations of the system at operating point.

Figure 1 shows a typical SMIB system including UPFC that consists of an excitation transformer (ET), a boosting transformer (BT), two three-phase GTO-based voltage source converters, and a DC link capacitor. Installed UPFC

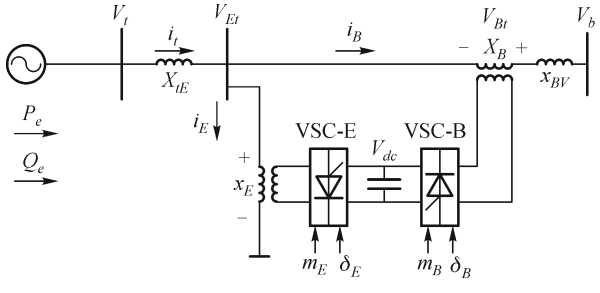

Fig. 1 A single machine connected to infinite bus with UPFC

is based on PWM converters and the control parameters of the UPFC are defined as following:

m_B: Amplitude modulation ratio related to the series inverter. With controlling of m_B, the amplitude of injected series voltage and compensator reactive power can be controlled.

δ_B: Phase angle of the series inverter that affects the transfer of active power.

m_E: Amplitude modulation ratio related to the parallel inverter. With controlling of m_E, voltage amplitude of UPFC bus and reactive power of the compensator can be controlled.

δ_E: Phase angle of the parallel inverter that sets the DC voltage related to DC link.

In order to consider the effects of UPFC in damping of the low-frequency swing (LFS), the dynamic model of the UPFC is employed, while the resistance and transient of the transformers of the UPFC can be disregarded. The equation describing the dynamic performance of the UPFC can be written as [26]

$$\begin{cases} \begin{bmatrix} V_{Etd} \\ V_{Etq} \end{bmatrix} = \begin{bmatrix} 0 & -x_E \\ x_E & 0 \end{bmatrix} \begin{bmatrix} i_{Ed} \\ i_{Eq} \end{bmatrix} + \begin{bmatrix} \dfrac{m_E \cos\delta_E V_{dc}}{2} \\ \dfrac{m_E \sin\delta_E V_{dc}}{2} \end{bmatrix}, \\ \begin{bmatrix} V_{Btd} \\ V_{Btq} \end{bmatrix} = \begin{bmatrix} 0 & -x_B \\ x_B & 0 \end{bmatrix} \begin{bmatrix} i_{Bd} \\ i_{Bq} \end{bmatrix} + \begin{bmatrix} \dfrac{m_B \cos\delta_B V_{dc}}{2} \\ \dfrac{m_B \sin\delta_B V_{dc}}{2} \end{bmatrix}, \end{cases} \tag{1}$$

$$\frac{\mathrm{d}V_{dc}}{\mathrm{d}t} = \frac{3m_E}{4C_{dc}} \begin{bmatrix} \cos\delta_E & \sin\delta_E \end{bmatrix} \begin{bmatrix} i_{Ed} \\ i_{Eq} \end{bmatrix} + \frac{3m_B}{4C_{dc}} \begin{bmatrix} \cos\delta_B & \sin\delta_B \end{bmatrix} \begin{bmatrix} i_{Bd} \\ i_{Bq} \end{bmatrix}. \tag{2}$$

The dynamic model of the power system presented in Fig. 1 is [26]

$$\dot{\delta} = \omega_0 \omega, \tag{3}$$

$$\dot{\omega} = \frac{P_m - P_e - D\omega}{M}, \tag{4}$$

$$\dot{E}'_q = \frac{-E_q + E_{fd}}{T'_{do}}, \tag{5}$$

$$\dot{E}_{fd} = \frac{-1}{T_A} E_{fd} + \frac{k_A}{T_A}(V_{t0} - V_t + u_{PSS}), \tag{6}$$

$$P_e = V_{td} i_{td} + V_{tq} i_{tq}, \tag{7}$$

$$V_t^2 = V_{td}^2 + V_{tq}^2, \tag{8}$$

$$\begin{cases} i_{Ed} = \dfrac{x_{BB}}{x_{d\Sigma}} E'_q - \dfrac{m_E \sin\delta_E V_{dc} x_{Bd}}{2x_{d\Sigma}} \\ \qquad + \dfrac{x_{dE}}{x_{d\Sigma}} \left(V_b \cos\delta + \dfrac{m_B \sin\delta_B V_{dc}}{2} \right), \\ i_{Eq} = \dfrac{m_E \cos\delta_E V_{dc} x_{Bq}}{2x_{q\Sigma}} + \dfrac{x_{qE}}{x_{q\Sigma}} \left(V_b \sin\delta + \dfrac{m_B \cos\delta_B V_{dc}}{2} \right), \\ i_{Bd} = -\dfrac{x_{dt}}{x_{d\Sigma}} \left(V_b \cos\delta + \dfrac{m_B \sin\delta_B V_{dc}}{2} \right) \\ \qquad + \dfrac{m_E \sin\delta_E V_{dc} x_{dE}}{2x_{d\Sigma}} + \dfrac{x_E}{x_{d\Sigma}} E'_q, \\ i_{Bq} = -\dfrac{m_E \cos\delta_E V_{dc} x_{qE}}{2x_{q\Sigma}} - \dfrac{x_{qt}}{x_{q\Sigma}} \left(V_b \sin\delta + \dfrac{m_B \cos\delta_B V_{dc}}{2} \right). \end{cases} \tag{9}$$

By combining and linearizing Eqs. (1)–(9), the state variable equations of the power system equipped with the UPFC can be represented as

$$\dot{x} = Ax + Bu, \tag{10}$$

$$x = \begin{bmatrix} \Delta\delta & \Delta\omega & \Delta E'_q & \Delta E_{fd} & \Delta V_{dc} \end{bmatrix}^{\mathrm{T}},$$

$$u = \begin{bmatrix} \Delta u_{PSS} & \Delta m_E & \Delta\delta_E & \Delta m_B & \Delta\delta_B \end{bmatrix}^{\mathrm{T}},$$

$$A = \begin{bmatrix} 0 & \omega_0 & 0 & 0 & 0 \\ -\dfrac{k_1}{M} & -\dfrac{D}{M} & -\dfrac{k_2}{M} & 0 & -\dfrac{k_{pd}}{M} \\ -\dfrac{k_4}{T'_{do}} & 0 & -\dfrac{k_3}{T'_{do}} & \dfrac{1}{T'_{do}} & -\dfrac{k_{qd}}{T'_{do}} \\ -\dfrac{k_A k_5}{T_A} & 0 & -\dfrac{k_A k_6}{T_A} & -\dfrac{1}{T_A} & -\dfrac{k_A k_{vd}}{T_A} \\ k_7 & 0 & k_8 & 0 & -k_9 \end{bmatrix},$$

$$B = \begin{bmatrix} 0 & 0 & 0 & 0 & 0 \\ 0 & -\dfrac{k_{pe}}{M} & -\dfrac{k_{p\delta e}}{M} & -\dfrac{k_{pb}}{M} & -\dfrac{k_{p\delta b}}{M} \\ 0 & -\dfrac{k_{qe}}{T'_{do}} & -\dfrac{k_{q\delta e}}{T'_{do}} & -\dfrac{k_{qb}}{T'_{do}} & -\dfrac{k_{q\delta b}}{T'_{do}} \\ \dfrac{k_A}{T_A} & -\dfrac{k_A k_{ve}}{T_A} & -\dfrac{k_A k_{v\delta e}}{T_A} & -\dfrac{k_A k_{vb}}{T_A} & -\dfrac{k_A k_{v\delta b}}{T_A} \\ 0 & k_{ce} & k_{c\delta e} & k_{cb} & k_{c\delta b} \end{bmatrix},$$

$$\Delta P_e = k_1 \Delta\delta + k_2 \Delta E'_q + k_{pd} \Delta V_{dc} + k_{pe} \Delta m_E + k_{p\delta e} \Delta\delta_E + k_{pb} \Delta m_B + k_{p\delta b} \Delta\delta_B, \tag{11}$$

$$\Delta V_t = k_5\Delta\delta + k_6\Delta E'_q + k_{vd}\Delta V_{dc} + k_{ve}\Delta m_E + k_{v\delta e}\Delta\delta_E + k_{vb}\Delta m_B + k_{v\delta b}\Delta\delta_B, \quad (12)$$

where Δm_E, Δm_B, $\Delta\delta_E$, and $\Delta\delta_B$ are the deviation of input control signals of the UPFC as explained previously.

Reactive power of the system expressed in *d-q* coordinates are obtained as

$$Q_e = V_{td}i_{tq} - V_{tq}i_{td}. \quad (13)$$

The voltage equations in *d-q* coordinates can be written as

$$V_{tq} = E'_q - x'_d i_{td}, \quad (14)$$

$$V_{td} = x_q i_{tq}. \quad (15)$$

Substituting Eqs. (14) and (15) into Eq. (13), we obtain

$$Q_e = (x_q i_{tq})i_{tq} - (E'_q - x'_d i_{td})i_{td}. \quad (16)$$

By linearizing Eq. (16), we have

$$\Delta Q_e = 2x_q i_{tq}\Delta i_{tq} - \Delta E'_q i_{td} - E'_q\Delta i_{td} + 2x'_d i_{td}\Delta i_{td}. \quad (17)$$

Finally,

$$\Delta Q_e = k_{10}\Delta\delta + k_{11}\Delta E'_q + k_{12}\Delta v_{dc} + k_{13}\Delta m_E + k_{14}\Delta\delta_E + k_{15}\Delta m_B + k_{16}\Delta\delta_B. \quad (18)$$

3 UPFC damping controller

To produce an electrical torque in phase with the speed deviation, the damping controller is designed according to phase compensation method. The four control parameters of the UPFC (m_E, m_B, δ_E, and δ_B) can be modulated in order to produce the damping torque. The construction of UPFC-based damping controller is similar to the PSS controllers as shown in Fig. 2. It consists of a gain block with gain G, a washout block with time constant T_ω, and a two-stage phase compensation block with time constant T_1, T_2, T_3, and T_4. The time constant T_d represents the finite delay caused by the firing controls and the natural response of the UPFC. In order to preserve the power equality between the series converters and the shunt converters, a DC link voltage regulator must be united where the DC voltage regulator is a PI-controller with the proportional and integral gains as K_{PDC} and K_{IDC}, respectively.

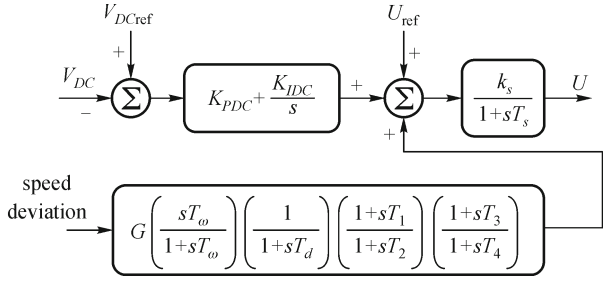

Fig. 2 Structure of UPFC-based damping controller

4 Dual-input PSS

Power system stability can be improved by damping the swing modes with suitably tuned power system stabilizers. Adequate tuned power system stabilizer will produce a control signal in phase with generator rotor speed deviation that causes damping of low frequency swing in participating generators. The input of PSS can be one of the local signals as generator speed deviation, accelerating power, or any other appropriate signal. These stabilizers by using lead-lag compensator or any other compensator create a portion of electrical torque in phase with generator rotor speed deviation. Among generator exciter control procedures for stability enhancement, PSS-based active power as the input signal is used in numerous cases. These procedures put down the local power swings between generators. With regard to the minor information contained in active power signal, the damping of low frequency power system swings is non-significant by this procedure. To solve this disadvantage of conventional PSS, rotor speed deviation as input signal is used [3,4,27,28]. These two signals, after crossing of the compensators, are gathered and the resultant signal is applied to PSS that can vastly improve stability. Therewith, voltage and reactive power are employed instead of the speed signal. Since frequency signal or speed signal can be computed and detected from the voltage and current; therefore, there is no need for tools with electromagnetic sensors.

The $p+\omega$ input PSS is shown in Fig. 3. p and ω are generator local signals which are selected as the PSS inputs. If p input PSS and ω input PSS are optimized independently and combined to make as $p+\omega$ input of PSS, an unexpected unstable swing mode may occur. In this paper, the parameters of the $p+\omega$ input of PSS with parameters of the UPFC controller are optimized all together.

The other model of the dual-input stabilizer described in IEEE Std 421.5 [6] is PSS2B (as shown in Fig. 4), which uses combinations of power and speed or frequency to derive the stabilizing signal. In this type of PSS, in order to extract a signal proportional to rotor speed deviation, the following equation is used:

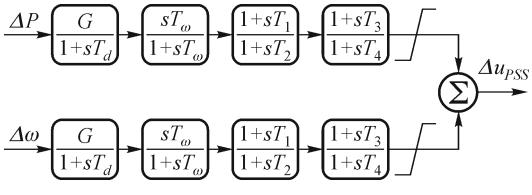

Fig. 3 Dual-input PSS

$$\Delta\omega_{eq} = \frac{1}{M}\int(\Delta P_m - \Delta P_e)\mathrm{d}t. \tag{19}$$

The objective is to derive the equivalent speed signal $\Delta\omega_{eq}$ so that it does not contain torsional modes. Torsional modes are weakened in the integral of ΔP_e signal. The problem is to measure the integral of ΔP_m free of torsional modes. In many applications, the ΔP_m component is neglected. This is satisfactory, except when the mechanical power changes. Under such conditions, a spurious stabilizer output is produced if ΔP_e alone is used as the stabilizing signal. The integral of mechanical power is related to shaft speed and electrical power as following:

$$\int \Delta P_m \mathrm{d}t = M\Delta\omega + \int \Delta P_e \mathrm{d}t. \tag{20}$$

According to Eq. (20), the integral of mechanical power change can be acquired by adding signals proportional to shaft-speed change and integral of electrical power change. This signal will contain torsional swings unless a filter is used. In Fig. 4, the ramp-tracking filter is a low-pass filter as torsional filter. Also, this filter minimizes the PSS output deviation that occurs when the mechanical power is changing rapidly.

5 Function optimization

In a typical optimization problem, the aim is to find the values of controllable parameters determining the behavior of a system. Numerous implementations of the evolutionary algorithm can be found in the electric power system [29]. The flexibility of the evolutionary algorithms in identifying the optimization problem using reasonable description and objective function has better potential over the classical optimization techniques. For constituting of the objective function to obtain the best values of controller gains and time constants, the mathematical model and the detailed description of the system are required. In this paper, to obtain the best values of controller gains and time constants, the objective function and system constraints are formulated as follows:

$$\text{Min}\quad f(G_m,T_n) = af_1 + bf_2, \tag{21}$$

$$\text{s.t. } G_{m\min} \leqslant G_m \leqslant G_{m\max},\ T_{n\min} \leqslant T_n \leqslant T_{n\max},$$

where

$$f_1 = \sum_{j=1}^{N}\sum_{\xi_i \leqslant \xi_0}(\xi_0 - \xi_{i,j})^2 \quad \text{and} \quad f_2 = \sum_{j=1}^{N}\sum_{\sigma_i \geqslant \sigma_0}(\sigma_0 - \sigma_{i,j})^2. \tag{22}$$

$\sigma_{i,j}$ and $\xi_{i,j}$ are the real part and damping ratio of the ith eigenvalue in the jth operating point. σ_0 and ξ_0 are the desired minimum real part and damping ratio to be achieved. G_m and T_n are the optimization parameters and $f(G_m,T_n)$ is the objective function, where m and n are the total number of gains and time constants, respectively. The values of a and b are the weight factors for f_1 and f_2 with regard to optimal point. In this article, σ_0, ξ_0, a, and b are selected as –2, 1, 5, and 10, respectively. N is the total number of operating points that survey is carried out.

The PSO algorithm is employed to solve this optimization problem and search for an optimal set of power damping controller parameters. It is emphasized that with this procedure, robust stabilization, which enables to operate satisfactory over a wide-range of the operating conditions, is obtained. The optimization of the controller parameters is carried out by evaluating the objective cost function as given in Eq. (21) that consists of a multiple of the operating conditions.

Evolutionary algorithm can be applied to any problem that can be formulated as Eqs. (21) and (22). Genetic algorithm (GA) and PSO are counted as the evolutionary algorithm. Genetic algorithm is a heuristic search to acquire approximate solution to the optimization problem. This algorithm uses procedures inspired by evolutionary biology such as mutation, cross over, and natural selection. Notwithstanding GA acquires good solutions in hard search spaces; it has some disadvantages such as the tendency to converge toward local optima rather than global optimum of the problem, and it is hard to implement. PSO is another evolutionary algorithm that nonlinearity and dimension of the problem are not considerable in this algorithm. In order to converge to optimal solution, this algorithm can be accomplished in search space for solving the optimization problem as formulated in Eq. (21). Numerous evolutionary algorithm

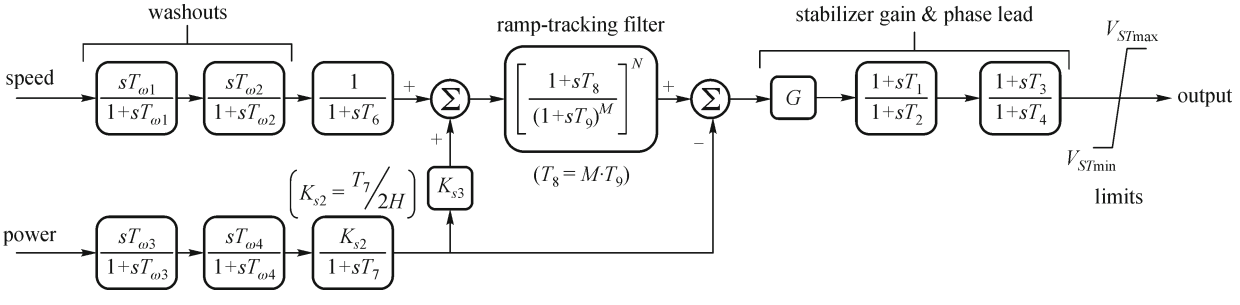

Fig. 4 PSS2B

applications, for parameter assessment to improve operation, can be found in electric power system publications [30–32]. Due to the following advantages of PSO, this algorithm has earned intensified attention among all optimization algorithms:

- It has the aptitude to escape local minima.
- Unlike other methods, it has a few parameters to adjust.
- It is comfortably implemented in computer coding.
- To start the iteration, it does not require to accurate initial solution.
- With almost any objective function, i.e., continuous or non-continuous, convex or non-convex, it can be used.
- It has more effective memory capability (local and neighboring best).

A detailed survey on PSO implementation in the large scale power system has been reviewed by Alrashidi and El-Hawary [33]. Furthermore, a comprehensive overview of PSO techniques and different applications in the electric power system are covered by del Valle et al. [34].

6 PSO algorithm

PSO algorithm is based on social behavior of birds. This method is proposed by Kennedy and Eberhart [35]. The main objective of their research is mathematical simulating the behavior of bird flocks. The objective is to find optimal areas in a complex search space with reciprocal action between populations of particles. Each individual of the population has an adoptable velocity (position change) related to particle movement in the search space. Moreover, each individual has a memory remembering the best position of the search space that it has met. Its movement is an accumulated acceleration toward its best previously visited position. Another best value that is traced by PSO is the best value earned so far by any particle in the neighborhood of the particle. The main idea is to modify the position and velocity of each particle toward the global best (g_{best}) position at each time stage. After the number of iterations, the particles among populations have been amassed around one or more of the optimal and tend to find the global optimal among all. In a system with given size and constraints, the solution is assumed to lie in the range of an N-dimensional space, where each potential solution is called a particle.

Stages of PSO algorithm is given as following:

Step 1 Initialize each particle with random solution in the problem sphere (initialization).

Step 2 Evaluate objective function for each particle.

Step 3 Calculate objective function and contrast it with its best particle (P_{best}). If the present value of the objective function is better than the P_{best}, then set the value as the P_{best} and the present position of the particle.

Step 4 The particle that has the best objective function value is distinguished among all the best particles. The value of objective function is assigned as g_{best} with its new position.

Step 5 For each particle, update the velocity vector and then the position vector according to

$$v_i^{k+1} = \omega v_i^k + c_1 r_1 (P_{id}^k - x_{id}^k) + c_2 r_2 (P_{gd}^k - x_{gd}^k), \quad (23)$$

$$x_{id}^{k+1} = x_{id}^k + c v_{id}^{k+1}. \quad (24)$$

The ith particle, the value of the competence for particle i, and the velocity of particle i is delineated as $X_i = (x_{i1},x_{i2},...,x_{iD})$, $P_i = (p_{i1},p_{i2},...,p_{iD})$, and $V_i = (v_{i1},v_{i2},...,v_{iD})$, sequentially. P_{id} and P_{gd} are P_{best} and g_{best}. The positive constants c_1 and c_2 are the cognitive and social components that are the acceleration constants liable for modifying the particle velocity towards P_{best} and g_{best}, respectively. Variables $r_1(\cdot)$ and $r_2(\cdot)$ are two random functions that generate uniformly distributed random numbers. The inertia weight ω creates a balance state between global search and local search; therefore, it decreases the number of iterations.

Step 6 Repeat Steps 2–5 until stopping criteria are met. These criteria are maximum iteration and minimum error criteria.

7 Controllability measurement

Singular value decomposition (SVD) is used to measure the ability of EM mode control with an input control signal [36]. SVD produces a diametrical matrix with dimension X where elements on the main diagonal of the matrix are non-negative and decreasing. Also, two matrices U and V are produced in which

$$x = USV. \quad (25)$$

For using of SVD in Matlab software, the follow equation is employed:

$$[U,S,V] = \text{svd}(x), \quad (26)$$

where $S = \text{svd}(x)$ gives the vector included singular value. Matrix B is introduced as $B = [\,b_1 \quad b_2 \quad b_3 \quad b_4 \quad b_5\,]$, where column b_i is related to the ith input. The smallest singular value $\delta_{\min}$ related to matrix $[\,\lambda_i I - A \quad b_i\,]$ shows the ability of the ith input for being controlled by λ. In fact, greater $\delta_{\min}$ is denoted as more capable of EM mode controllability. Therefore, we can find the value of EM mode controllability for the input that system has the greatest value of controllability. To measure the ability of EM mode control for each of the five inputs u_{PSS}, m_E, δ_E, m_B, and δ_B, the value of $\delta_{\min}$ is obtained over a wide range of operating conditions. For SVD analysis, as shown in Figs. 5–7, P_e changes from 0.05 to 1.4 and Q_e changes from –0.4 to 0.4. From these figures, it can be observed that the controllability of the different inputs of UPFC and PSS is increased with P_e increasing, and the controllability via

δ_E is always higher than that of any other input.

8 Simulation results

By using the linearized power system model and PSO algorithm, interactions among UPFC damping controller and dual-input PSS controller are considered, and the controller parameters are optimized simultaneously to achieve a global optimal damping behaviour. The eigenvalue analysis and the nonlinear time-domain simulation are used to validate the effectiveness of the proposed controller.

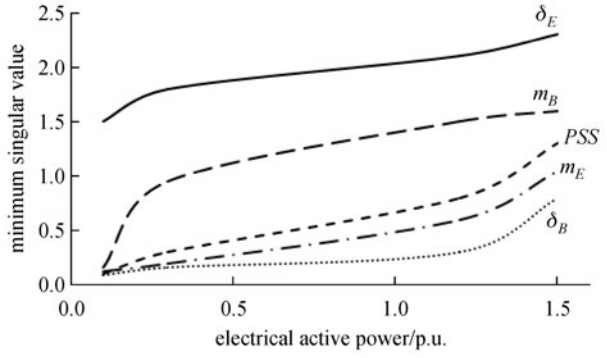

Fig. 5 Minimum singular value with all stabilizers at Q_e = –0.4 p.u.

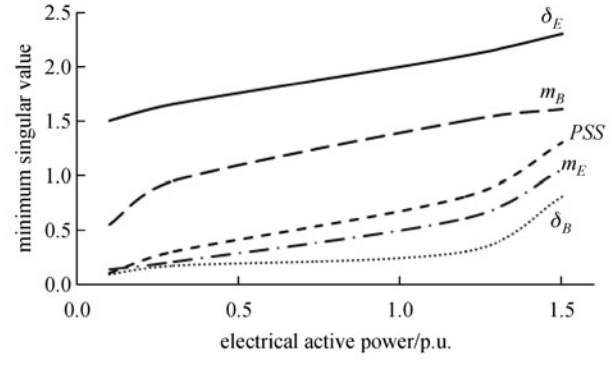

Fig. 6 Minimum singular value with all stabilizers at Q_e = 0.0 p.u.

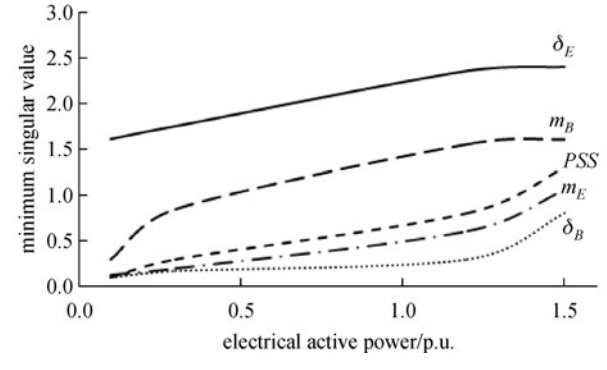

Fig. 7 Minimum singular value with all stabilizers at Q_e = 0.4 p.u.

8.1 Dominant eigenvalues

The eigenvalue analysis can be a quantitative method to evaluate the dynamic stability of power system in figure of damping ratio and damping constant or other stability measurement indices. In order to obtain robust controllers for SMIB system with data given in the Appendix, three different operating points representing light, nominal, and heavy (as given in Table 1) are taken into account in the design process. Figure 8 shows the convergence rate of the objective function where the various coordinated controllers have been optimized. It can be easily seen that the PSS2B & UPFC controller has been adjusted with the smallest cost value in comparison with other designs. This means that damping effect of the PSS2B & UPFC coordination may be the best.

The detailed controller parameters are given in Table 2. Also, at the three operating points, such as nominal, light, and heavy given in Table 1, the system eigenvalues for both cases, without and with the proposed stabilizers with $\xi < 1$, are given in Table 3. This table clearly demonstrates the effectiveness of the dual-input PSS and PSS2B coordination with UPFC in enhancing of system stability. After the coordinated tuning of dual-input PSS & UPFC and PSS2B & UPFC controllers, electromechanical modes of swings are well damped. The results show the

Table 1 Loading conditions

loading	P_e/p.u.	Q_e/p.u.
nominal	0.8	0.167
heavy	1.2	0.4
light	0.2	0.01

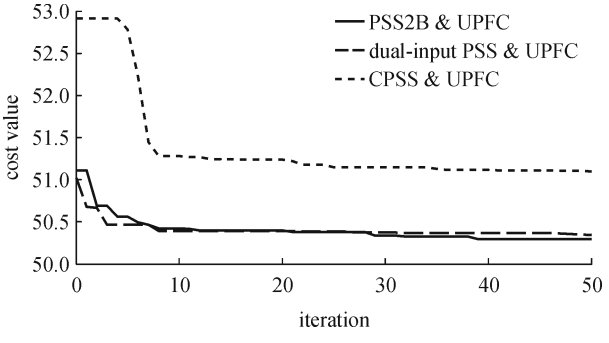

Fig. 8 Profiles of objective function

Table 2 Optimal parameters and settings of the proposed controllers

controller parameters	coordinated design		coordinated design			coordinated design	
	CPSS	UPFC	dual-input PSS		UPFC	PSS2B	UPFC
			ω input	P input			
G	100	7.1440	0.2690	0.1505	–17.5212	2.0069	8.4627
T_1	0.6324	0.2785	0.0646	0.8147	0.05	1.4940	0.4854
T_2	1.0073	0.8183	0.05	0.9058	1.0568	0.1576	0.8003
T_3	1.3639	0.5469	0.9575	0.1270	0.9649	0.9706	0.1419
T_4	0.975	1.0924	0.05	0.9134	0.9054	0.9572	0.4446

Table 3 Eigenvalues and damping ratios of power system before and after the coordinated tuning with $\xi < 1$

	nominal		heavy		light	
	eigenvalue	damping ratio	eigenvalue	damping ratio	eigenvalue	damping ratio
without PSS, dual-input PSS and UPFC	0.0773±i6.56 –0.179±i0.66	–0.0118 0.2609	0.0775±i6.37 –0.311±i0.82	–0.0122 0.3546	0.0713±i6.5243	–0.0109
CPSS & UPFC	–2±i2.65 –1.87±i2.13 –1.77±i1.37	0.6019 0.6596 0.7922	–2.74±i4.06 –1.5±i0.84 –1.18±i0.53 –1.07±i0.36	0.5593 0.8715 0.9115 0.9477	–1.99±i5.73 –1.59±i1.1	0.3277 0.8223
dual-input PSS & UPFC	–1.264±i5.25 –6.6±i1.55 –0.95±i0.11	0.9234 0.9736 0.9936	–9.45±i6.54 –3.15±i1.70 –11.93±i3.41 –0.95±i0.11	0.8221 0.8804 0.9614 0.9936	–5.35±i5.62 –4.63±i3.05 –0.79±i0.49	0.6896 0.8355 0.8512
PSS2B & UPFC	–12.64±5.25i –6.82±1.38i –0.95 – 0.11i –5.13±0.25i	0.9235 0.9802 0.9938 0.9988	–10.30±5.72i –7.77±3.05i –0.95±0.11i	0.8741 0.9310 0.9937	–2.98±2.98i –8.68±6.43i –12.85±4.51i	0.7073 0.8036 0.9435

improvement in damping of overall power swings in the system for which all the damping ratios are more than 50%.

8.2 Nonlinear simulation results

In order to illustrate the performance of the proposed controllers, simulation studies using MATLAB/Simulink are carried out as shown in Fig. 9 and is verified by applying a three-phase fault of 100 ms duration at the infinite bus in the test system at $t = 1$ s. To evaluate the performance of the proposed controllers, the responses of the coordinated tuning of the dual-input PSS & UPFC damping controller and PSS2B & UPFC damping controller are compared with the response of the coordinated tuning of the CPSS & UPFC damping controller. Figures 10 and 11 show the speed deviation and power deviation for the three loading conditions. It is clear from these figures that, the simultaneous design of the dual-input PSS & UPFC and PSS2B & UPFC damping controllers significantly improve the stability performance of the test power system, and low frequency swings are well damped out and the PSS2B & UPFC controller has the best performance.

9 Conclusion

The power system stability enhancement via coordination between dual-input PSS and FACTS-based stabilizers has been discussed and investigated for an SMIB system. Also, a comparative performance study of a single-input PSS, dual-input PSS, and PSS2B coordination with UPFC has been carried out to appreciate the effectiveness of dual-input PSS and PSS2B in contrast to CPSS. For the proposed controllers design problem, an objective function to minimize the power system swing has been used. Then, particle swarm optimization algorithm has been employed to optimally and coordinately tune the controller parameters. Simulation results have been presented for various loading conditions and disturbances to show the effectiveness of the proposed coordinated design. The proposed controllers are robust to fault in different operating conditions and generate appropriate stabilizing output control signals to improve stability. The simulation results show that the dual-input PSS & UPFC and PSS2B & UPFC coordination can more effectively damp the system swings under different operation conditions than the conventional single-input PSS & UPFC coordination. Also, the PSS2B & UPFC coordination has the best performance.

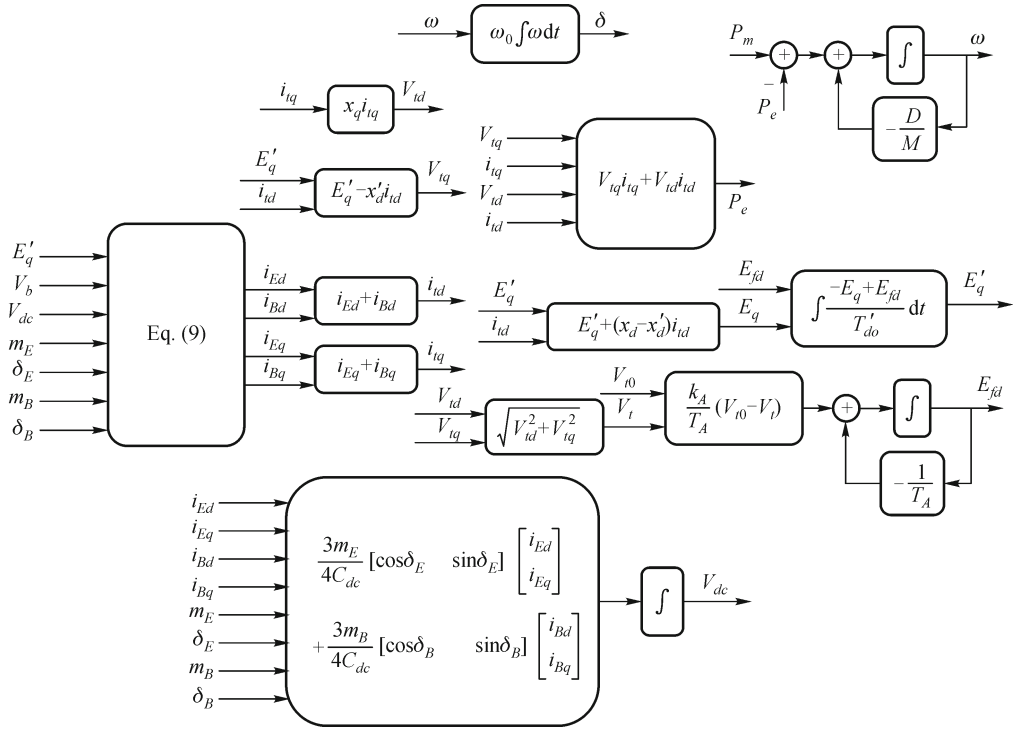

Fig. 9 Nonlinear simulation of test system

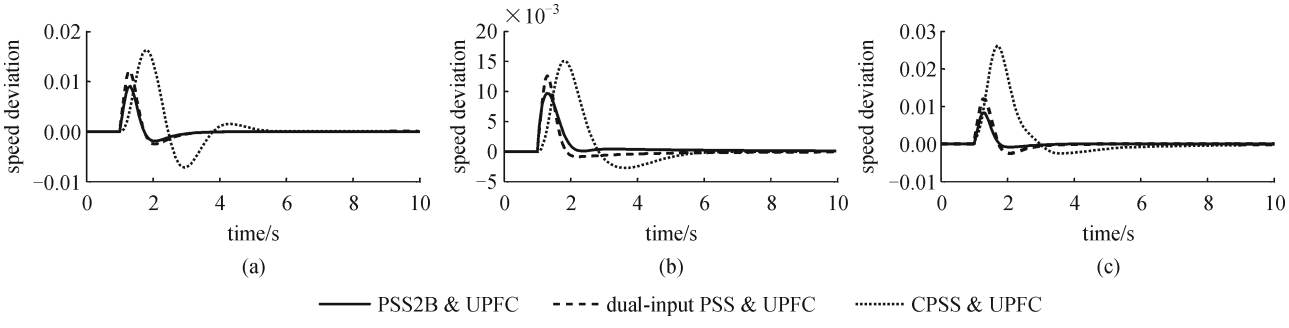

Fig. 10 Dynamic responses for speed deviation at (a) nominal, (b) heavy, and (c) light loading conditions. Solid line: PSS2B & UPFC, dashed line: dual-input PSS & UPFC, dotted line: CPSS & UPFC

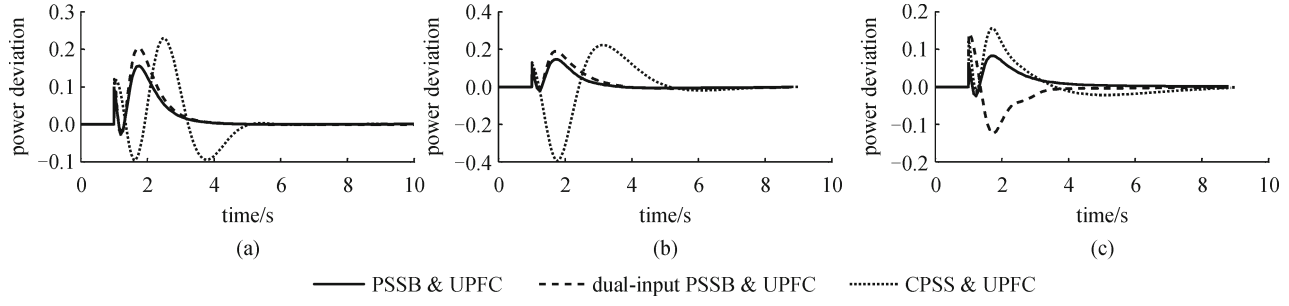

Fig. 11 Dynamic responses for active power deviation at (a) nominal, (b) heavy, and (c) light loading conditions. Solid line: PSS2B & UPFC, dashed line: dual-input PSS & UPFC, dotted line: CPSS & UPFC

Appendix A

SMIB system data:

- Machine: $H = 6.5$; $T'_{do} = 8.0$ s; $D = 0$; $x'_d = 0.3$; $x_q = 0.6$; $x_d = 1.8$; $f = 60$; $v = 1.05$.
- Exciter: $k_A = 20$; $T_A = 0.05$.
- Dual-input PSS: $T_w = 10$; $T_{i\min} = 0.05$; $T_{i\max} = 1.5$; $i = 1, 2, 3, 4$; $G_{\min} = -100$; $G_{\max} = 100$; $T_d = 0.01$.
- PSS2B: $T_{w1} = 10$; $T_{w2} = 10$; $T_{w3} = 10$; $T_{w4} = 0$; $T_6 = 0$; $T_7 = 10$; $K_{s3} = 1$; $K_{s2} = T_7/H$; $M = 5$; $N = 1$.
- Transmission line: $x_{tE} = 0.1$; $x_{BV} = 0.6$.
- UPFC: $x_E = 0.1$; $x_B = 0.1$; $K_s = 1$; $T_s = 0.05$; $C_{DC} = 3$; $K_{PDC} = -11$; $K_{IDC} = 0$; $V_{dc} = 2$; $m_{E\min} = 0$; $m_{E\max} = 2$; $m_{B\min} = 0$; $m_{B\max} = 2$; $T_w = 10$; $T_d = 0.01$; $T_{i\min} = 0.05$; $T_{i\max} = 1.5$; $G_{\min} = -100$; $G_{\max} = 100$; $i = 1, 2, 3, 4$.

References

1. Kundur P, Balu N J, Lauby M G. Power System Stability and Control. New York: McGraw-Hill, 1994
2. Rogers G. Power System Oscillations. Boston: Kluwer Academic, 2000
3. Kitauchi Y, Taniguchi H, Shirasaki T, Ichikawa Y, Amano M, Banjo M. Experimental verification of multi-input PSS with reactive power input for damping low frequency power swing. IEEE Transactions on Energy Conversion, 1999, 14(4): 1124–1130
4. Kamwa I, Grondin R, Trudel G. IEEE PSS2B versus PSS4B: The limits of performance of modern power system stabilizers. IEEE Transactions on Power Systems, 2005, 20(2): 903–915
5. Liu Y, Li J, Li C. Robust excitation control of multi-machine multi-load power systems using Hamiltonian function method. Frontiers of Electrical and Electronic Engineering in China, 2011, 6(4): 547–555
6. IEEE Power Engineering Society. IEEE Recommended Practice for Excitation System Models for Power System Stability Studies (IEEE Std 421.5-2005). 2006
7. Shakarami M R, Kazemi A. Robust design of static synchronous series compensator-based stabilizer for damping inter-area oscillations using quadratic mathematical programming. Journal of Zhejiang University—Science C, 2010, 11(4): 296–306
8. Chang J, Chow J H. Time-optimal series capacitor control for damping interarea modes in interconnected power systems. IEEE Transactions on Power Systems, 1997, 12(1): 215–221
9. Abido M A. Genetic-based TCSC damping controller design for power system stability enhancement. In: Proceedings of International Conference on Electric Power Engineering. 1999, 165
10. Abido M. Pole placement technique for PSS and TCSC-based stabilizer design using simulated annealing. International Journal of Electrical Power & Energy Systems, 2000, 22(8): 543–554
11. Rezazadeh A, Sedighizadeh M, Hasaninia A. Coordination of PSS and TCSC controller using modified particle swarm optimization algorithm to improve power system dynamic performance. Journal of Zhejiang University—Science C, 2010, 11(8): 645–653
12. Baker R, Guth G, Egli W, Eglin P. Control algorithm for a static phase shifting transformer to enhance transient and dynamic stability of large power systems. IEEE Transactions on Power Apparatus and Systems, 1982, PAS-101(9): 3532–3542
13. Jiang F, Choi S, Shrestha G. Power system stability enhancement using static phase shifter. IEEE Transactions on Power Systems, 1997, 12(1): 207–214
14. Jiang T, Chen C, Cao G. Nonlinear optimal predictive controller for static var compensator to improve power system damping and to maintain voltage. Frontiers of Electrical and Electronic Engineering in China, 2006, 1(4): 380–384
15. Sun L Y, Tong S, Liu Y. Adaptive backstepping sliding mode H_∞ control of static var compensator. IEEE Transactions on Control Systems Technology, 2011, 19(5): 1178–1185
16. Rao P S, Sen I. A QFT based robust SVC controller for improving the dynamic stability of power systems. In: Proceedings of the Fourth International Conference on Advances in Power System Control, Operation and Management. 1997, 1: 366–370
17. Parniani M, Iravani M. Optimal robust control design of static VAR compensators. IEE Proceedings—Generation, Transmission and Distribution, 1998, 145(3): 301–307
18. Jalilvand A, Safari A. Design of an immune-genetic algorithm-based optimal state feedback controller as UPFC. In: Proceedings of the 6th International Conference on Electrical Engineering/Electronics, Computer, Telecommunications and Information Technology. 2009, 36–39
19. Dash P, Mishra S, Panda G. Damping multimodal power system oscillation using a hybrid fuzzy controller for series connected FACTS devices. IEEE Transactions on Power Systems, 2000, 15(4): 1360–1366
20. Dong L, Zhang L, Crow M. A new control strategy for the unified power flow controller. In: Proceedings of the IEEE Power Engineering Society Winter Meeting. 2002, 1: 562–566
21. Schoder K, Hasanovic A, Feliachi A. Fuzzy damping controller for the unified power flow controller. In: Proceedings of the IEEE Power Engineering Society Winter Meeting. 2000, 5–21
22. Nguyen T, Gianto R. Neural networks for adaptive control coordination of PSSs and FACTS devices in multimachine power system. IET Generation, Transmission & Distribution, 2008, 2(3): 355–372
23. Lei X, Lerch E N, Povh D. Optimization and coordination of damping controls for improving system dynamic performance. IEEE Transactions on Power Systems, 2001, 16(3): 473–480
24. Cai L J, Erlich I. Simultaneous coordinated tuning of PSS and FACTS damping controllers in large power systems. IEEE Transactions on Power Systems, 2005, 20(1): 294–300
25. Pourbeik P, Gibbard M J. Simultaneous coordination of power system stabilizers and FACTS device stabilizers in a multimachine power system for enhancing dynamic performance. IEEE Transactions on Power Systems, 1998, 13(2): 473–479
26. Wang H. Damping function of unified power flow controller. IEE Proceedings—Generation, Transmission and Distribution, 1999, 146(1): 81–87
27. Yoshimura K, Uchida N. Multi input PSS optimization method for practical use by considering several operating conditions. In: Proceedings of the IEEE Power Engineering Society Winter

Meeting. 1999, 749–754
28. Hashemi Y, Kazemzadeh R, Azizian M R, Sadeghi A, Morsali J. Simultaneous coordinated tuning of UPFC and multi-input PSS for damping of power system oscillations. In: Proceedings of the 26th International Power System Conference. 2011
29. Alves da Silva A, Abrão P J. Applications of evolutionary computation in electric power systems. In: Proceedings of the Congress on Evolutionary Computation. 2002, 1057–1062
30. Abdel-Magid Y, Abido M. Optimal multiobjective design of robust power system stabilizers using genetic algorithms. IEEE Transactions on Power Systems, 2003, 18(3): 1125–1132
31. Do Bomfim A L B, Taranto G N, Falcao D M. Simultaneous tuning of power system damping controllers using genetic algorithms. IEEE Transactions on Power Systems, 2000, 15(1): 163–169
32. Jayabarathi T, Bahl P, Ohri H, Yazdani A, Ramesh V. A hybrid BFA-PSO algorithm for economic dispatch with valve-point effects. Frontiers in Energy, 2012, 6(2): 155–163
33. Alrashidi M, El-Hawary M. A survey of particle swarm optimization applications in power system operations. Electric Power Components and Systems, 2006, 34(12): 1349–1357
34. del Valle Y, Venayagamoorthy G K, Mohagheghi S, Hernandez J C, Harley R G. Particle swarm optimization: Basic concepts, variants and applications in power systems. IEEE Transactions on Evolutionary Computation, 2008, 12(2): 171–195
35. Kennedy J, Eberhart R. Particle swarm optimization. In: Proceedings of International Conference on Neural Networks. 1995, 1942–1948
36. Hamdan A. An investigation of the significance of singular value decomposition in power system dynamics. International Journal of Electrical Power & Energy Systems, 1999, 21(6): 417–424